IN SITU MONITORING AND MODELLING OF PITTING CORROSION ON 2024 ALUMINUM ALLOY

J.M. OLIVE *, S. CABROL * and T. JASZAY **

* Laboratoire de Mécanique Physique, Université Bordeaux I, 351 Cours de la Libération, 33405 Talence cedex, France.
** Laboratoire de Mécanique des fluides, Ecole Centrale de Nantes, 1, rue de la Noë, 44072 Nantes, France

ABSTRACT Localized corrosion in the form of pitting is recognized as one of the degradation processes that affect the durability of structures. In a 2024-T3 aluminum alloy, pitting was observed to nucleate and develop at constituent particles, which are either anodic or cathodic relative to the matrix. Two modes of pitting were identified : pitting associated with the galvanic coupling between matrix and isolated particle ; and severe pitting that results from the interaction with a cluster of cathodic particle. A mechanistic model of severe pitting based on galvanic corrosion and results of simulation are presented.

Keywords : *alluminum alloy, pitting corrosion, modelling, numerical simulation*

1. INTRODUCTION

High strength aluminium alloys are susceptible to corrosion and corrosion fatigue that can compromise the integrity of structures. Microstructural heterogeneities such as constituent particles play a major role in the localized corrosion for these alloys [1,3]. The mechanism involved in the developpement of localized corrosion on 2024 T3 alloy is the galvanic coupling between constituent particles and the matrix [4]. Two types of particles were identified ; one containing Al, Cu and Mg acting as anode versus the matrix and the other, Al, Cu, Mn and Fe acting as cathode relative to the matrix. Twenty-five percent of the overall particles (3,000 mm^{-2}) are cathodic and banding and clustering along the rolling direction is evident.

In situ monitoring of pitting process on 2024 T3 in 0.5 M NaCl was performed using long focal length video microscopy [5]. Two modes of pitting corrosion were identified : namely, (i) pitting associated with single particles, and (ii) severe pitting resulting from growth in depth of corrosion cavities at selected sites. Because severe pits are potential sites for corrosion fatigue crack initiation, emphasis is placed herein on the mechanistic understanding and modelling of this process. Probabilistic modelling for the growth of corrosion pits taking into account the role of clustered particles was proposed [6]. Three different models with increasing complexity relative to geometrical assumptions on the shape of corrosion cavities were detailed. A lack in mechanistic understanding was apparent. A mechanistic model fully based on galvanic corrosion is presented here.

2. DEVELOPMENT OF THE MODEL

The corrosion process considered in this model is the galvanic coupling between constituent particles and the matrix. The first step consists on the measure and the modelling of the growth of pitting associated with a single particle. This is the basis of the severe pit modelling since a galvanic current as a function of the cathodic to anodic surface areas ratio is obtained. The second step is the assessment of the anodic and cathodic surface areas during the propagation of the severe pit through

the particle cluster. The growth kinetics are then evaluated from the knowledge of the galvanic current inferred from the first step result.

2.1 Pitting associated with single particles

This is a typical problem of galvanic corrosion where two media of different electrochemical characters are in contact. Several investigations on accelerated corrosion of dissimilar metals which are electrically coupled and exposed to a corrosive environment were reported [7-12]. Based on general theory of galvanic corrosion [10, 11], the dependence of the anodic and cathodic galvanic current densities and the galvanic potential on the cathodic to anodic surface ratio areas were derived. The calculation, however, required a knowledge of electrochemical character of each uncoupled metal and considered only coplanar electrodes. For galvanic corrosion between constituent particles and the matrix, the pit morphology led to geometrical changes of anodic and cathodic surfaces with time. Furthermore, electrochemical behavior of uncoupled particles and matrix are not known. The evaluation of galvanic current, cathodic and anodic surface areas must be then approach experimentally by making some assumptions on the pit geometry. This is illustrated in a flow diagram presented in figure 1.

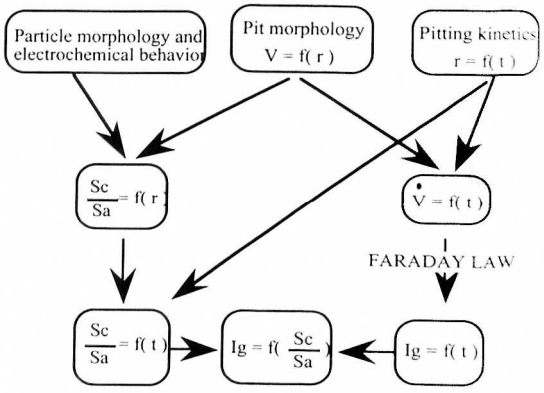

Fig. 1. Quantitative assessment of the galvanic current between constituent particle and matrix. V : pit volume, r : pit radius, Sc : cathodic surface area, Sa : anodic surface area, Ig : galvanic current.

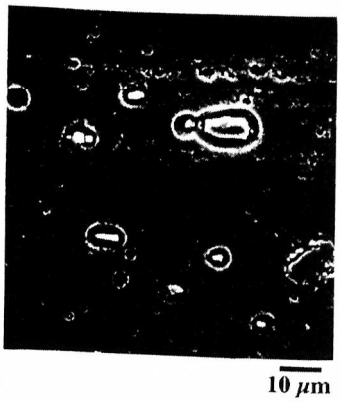

Fig. 2. Corrosion pitting resulting from galvanic coupling between cathodic particle and the matrix. 2024 T3 alloy in 0.5 M NaCl at free corrosion potential

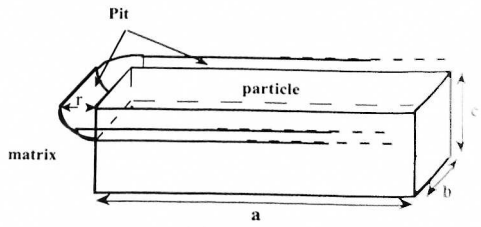

Fig. 3. Pit morphology associated to a cathodic constituent particle.

Particle morphology and its electrochemical behavior were obtained after a corrosion test and removal of corrosion products. The scanning electron microscopy picture presented in figure 2 shows typical pitting produced by galvanic coupling between cathodic particle and matrix.

From this observation, a model of pitting (figure 3) associated with single particle is proposed making the following assumptions : (1) Cathodic particle is a rectangular prism with the dimension along the rolling direction being higher than those in the transverse and short directions, (2) Pit initiation occurs at the particle-matrix interface, (3) Anodic dissolution of the matrix is isotropic, (4) The cathodic surface where reduction reaction occurs is the particle surface in contact with the electrolyte. The anodic surface is the substrate surface of the pit.

The dimensions of the particle along the rolling, transverse and short directions are respectively a, b and c. The pit size is given by r. For $r \leq c$, the cathodic and anodic surface areas as well as the pit volume are easily obtained :

$$\text{For } r \leq c, \quad \begin{aligned} S_c &= a\,b + 2\,r\,(a+b) \\ S_a &= \pi\,r\,(a+b+2\,r) \\ V_{pit} &= \pi\,r^2\left(\frac{a+b}{2} + \frac{2\,r}{3}\right) \end{aligned} \qquad (1)$$

The pitting kinetics in terms of r = f(t) needs to be measured experimentally. In situ monitoring of the pitting process was performed during corrosion test by using long focal length video microscopy. A particle with a rectangular shape was chosen before immersion of the specimen and r was measured. Picture presented in figure 4 show the shape of the cathodic constituent particle and the pit growth 16 h after immersion.

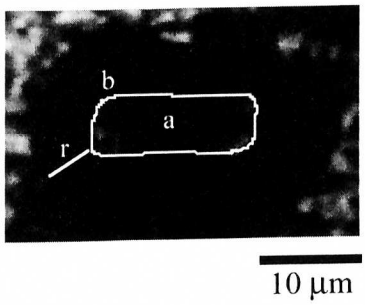

Fig. 4. In situ monitoring of corrosion pitting (b) resulting from galvanic coupling between cathodic particle (a) and the matrix. 2024 T3 alloy in 0.5 M NaCl at free corrosion potential, 16 h after immersion.

The pit size r was measured continuously from immersion to 17 h and could be expressed according to time t (in secondes) by :

$$r = 6.10^{-8}\,t^{0.45} \qquad (2)$$

From Eq. (1) and Eq. (2), S_c , S_a in m^2 and V_{pit} in m^3 are deduced as a function of time in secondes, the particle dimensions a and b being respectively 17.10^{-6} m and 6.10^{-6} m :

$$\begin{aligned} S_c &= 10^{-10} + 276\,10^{-14}\,t^{0.45} \\ S_a &= 2.7.10^{-12}\,t^{0.53} \\ V_{pit} &= 9.10^{-20}\,t^{0.95} \end{aligned} \qquad (3)$$

From V(t), the galvanic current Ig (in amperes) associated to the anodic dissolution of the matrix surrounding the cathodic particle is obtained by the Faraday law :

$$I_g = \frac{n \rho F}{M} \frac{\partial V}{\partial t} \qquad (4)$$

where M is the molecular weight of the alloy (M = 27 g/mol), n the valence of oxidized spec (n = 3), F the Faraday constant (F = 96,514 C/mol) and ρ the density (ρ = 2.7 10^6 g/m^3).

Consequently, from Eq. (3) and Eq. (4) the expression of I_g can be approximated versus th ratio cathodic to anodic surface areas as :

$$I_g = 1.7 . 10^{-9} + 5. 10^{-10} \log \frac{S_c}{S_a} \qquad (5)$$

This quantitative assessment of the galvanic current as a function of surface areas is used the severe pitting model described in the following section.

2.2 Severe pitting model

Severe pitting is clearly associated with clustering of type cathodic particles. It can be not that the severe pitting surface density is very low according to that of pitting on single particle After 20 hr of a corrosion test, the severe pit density is about 1.5 pit.mm^{-2}. The approach aims modelize the growth of this severe pit in a particle cluster, the postulated driving force being th galvanic coupling between particles and matrix. Only the general features of the model are presente in this section, numerical computations are currently performed and the results will be presente later.

Morphological observations of severe pits after corrosion test showed that their shape co be approximate by a rectangular prism (figure 5).The dimension A along the rolling direction is most of the case higher than B and C, and the side 6 is the mouth of the pit. Severe pit propagates a particle cluster. Therefore, at each time t of the propagation, the cavity sides intersect cathod particles of the cluster. It is then possible to compute the cathodic and anodic surface areas on ea side of the pit at time t.

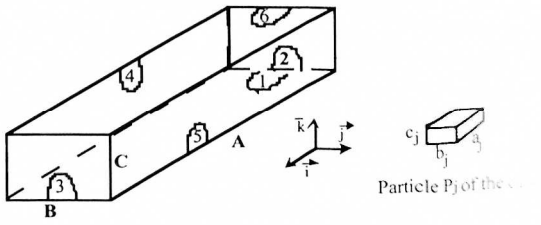

Fig. 5. Severe pit and particle shape considered in the model.

The total cathodic surface area S_{c1} on side 1, is then given by :

$$S_{c1} = \sum_{1}^{n} S_{1j}$$

with S_{1j} given by :

$$S_{1j} = \left\{ \left(\frac{c_j}{2} - \overline{l_{1j}}\right) \left\{ \left[b_j - \left(\frac{b_j}{2} - \overline{l_{5j}}\right) H\left(\frac{b_j}{2} - \overline{l_{5j}}\right) - \left(\frac{b_j}{2} + \overline{l_{4j}}\right) H\left(\frac{b_j}{2} + \overline{l_{4j}}\right) \right] \left[H\left(-\overline{l_{2j}} - \frac{a_j}{2}\right) + H\left(\overline{l_{3j}} - \frac{a_j}{2}\right) \right] + \left[a_j - \left(\frac{a_j}{2} + \overline{l_{2j}}\right) H\left(\frac{a_j}{2} + \overline{l_{2j}}\right) - \left(\frac{a_j}{2} - \overline{l_{3j}}\right) H\left(\frac{a_j}{2} - \overline{l_{3j}}\right) \right] \left[H\left(\overline{l_{5j}} - \frac{b_j}{2}\right) + H\left(-\frac{b_j}{2} - \overline{l_{4j}}\right) \right] \right\} + \left[b_j - \left(\frac{b_j}{2} - \overline{l_{5j}}\right) \right.$$

$$H\left(\frac{b_j}{2} - \overline{l_{5j}}\right) - \left(\frac{b_j}{2} + \overline{l_{4j}}\right) H\left(\frac{b_j}{2} + \overline{l_{4j}}\right)\Big]\Big[a_j - \left(\frac{a_j}{2} + \overline{l_{2j}}\right) H\left(\frac{a_j}{2} + \overline{l_{2j}}\right) - \left(\frac{a_j}{2} - \overline{l_{3j}}\right) H\left(\frac{a_j}{2} - \overline{l_{3j}}\right)\Big]\Big\} H\left(\frac{c_j}{2} - \overline{l_{1j}}\right)$$
$$H\left(\frac{c_j}{2} + \overline{l_{1j}}\right) H\left(\frac{b_j}{2} + \overline{l_{5j}}\right) H\left(\frac{b_j}{2} - \overline{l_{4j}}\right) H\left(\frac{a_j}{2} + \overline{l_{3j}}\right) H\left(\frac{a_j}{2} - \overline{l_{2j}}\right)$$

with $H(x) = \begin{cases} 1 \text{ for } x > 0 \\ 0 \text{ for } x \leq 0 \end{cases}$ and $\overline{l_{ij}}$, the algebric distance between the particule P_j centroid and the face S_i of the severe pit.

The anodic surface area S_{a1} is obtained by :

$$S_{a1} = S_1 - S_{ps1}$$

with S_1 the total surface area of the side S_1 and S_{ps1}, the total surface area of the particle sections on side S_1.

S_{ps1} is given by :

$$S_{ps1} = \sum_{j=1}^{n} [b_j - \left(\frac{b_j}{2} - \overline{l_{5j}}\right) H\left(\frac{b_j}{2} - \overline{l_{5j}}\right) - \left(\frac{b_j}{2} + \overline{l_{4j}}\right) H\left(\frac{b_j}{2} + \overline{l_{4j}}\right)]\Big[a_j - \left(\frac{a_j}{2} + \overline{l_{2j}}\right) H\left(\frac{a_j}{2} + \overline{l_{2j}}\right) - \left(\frac{a_j}{2} - \overline{l_{3j}}\right)$$
$$H\left(\frac{a_j}{2} - \overline{l_{3j}}\right)\Big] H\left(\frac{c_j}{2} - \overline{l_{1j}}\right) H\left(\frac{c_j}{2} + \overline{l_{1j}}\right) H\left(\frac{b_j}{2} + \overline{l_{5j}}\right) H\left(\frac{b_j}{2} - \overline{l_{4j}}\right) H\left(\frac{a_j}{2} + \overline{l_{3j}}\right) H\left(\frac{a_j}{2} - \overline{l_{2j}}\right)$$

From this information and Eq. (5), the propagation rate of side 1 $\left.\frac{\partial r}{\partial t}\right|_1$ is given by :

$$\left.\frac{\partial r}{\partial t}\right|_1 = \frac{M}{n \rho F} \frac{I_g}{S_{a1}}$$

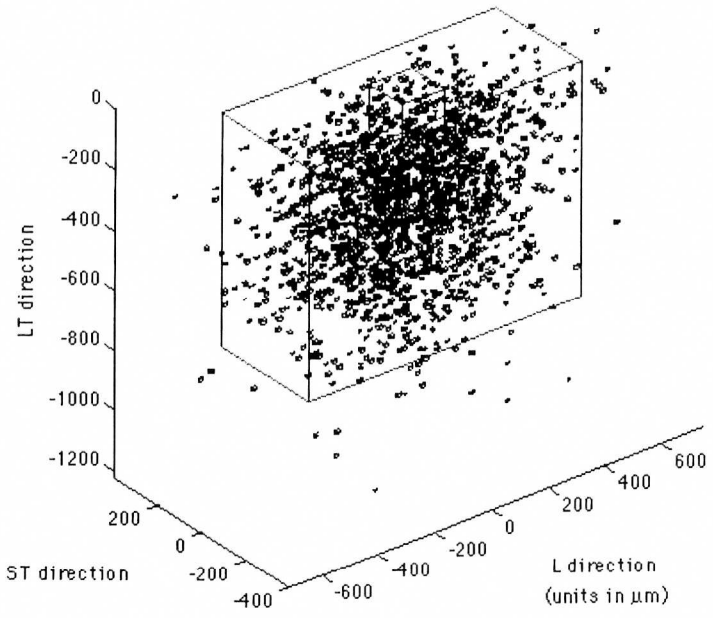

Fig. 7 : Simulation of severe pit growth through a cluster of 1800 cathodic particles.

The propagation rate of each side of the severe pit is computed step by step. The diffe steps of the numerical simulation are : (1) generation of the cathodic particle cluster coherent v statistical analysis of particle distribution (truncated by the interface metal-electrolyte and elong in the rolling direction), (2) definition of the initial cavity for severe pit initiation, (3) computat the cathodic and anodic surface areas on each side of the pit, (4) computation of propagation rat each side.

The program was written under the sofware MATLAB (Scientific Software Gro Simulation of severe pit growth through a cluster of 1,800 particles is shown in Fig. 7. Initial ca and the cavity after 8,321 iterations corresponding to 2,311 hours in real time are described average computed growth rate in LT direction (for the first 48 hours of propagation) is ar $6.5.10^{-10}$ $m.s^{-1}$ that is the same order of magnitude than the experimental growth ($8.3.10^{-10}$ $m.s^{-1}$). The other average computed growth rates in ST and L directions are respecti $0.8.10^{-10}$ $m.s^{-1}$ and $7.7.10^{-10}$ $m.s^{-1}$. The corresponding experimental rates are $2.2.10^{-10}$ m.s 17.10^{-10} $m.s^{-1}$.

The influence of particles distribution and morphology on the pit growth anisotrop currently studied by making computations on clusters containing cubic particles and /or elonga along the rolling direction.

3. CONCLUSION

A mechanistic model for severe pitting on 2024 T3 alloy is proposed. The mechanism of growth considered is the galvanic coupling between cathodic constituent particles and the mat From in situ monitoring of pitting process by video microscopy and some assumptions the galv current is given as a function of the cathodic and anodic surface areas. This galvanic current is u in a mechanistic model to compute the growth rate of severe. Preliminary numerical simulation the severe pitting model are presented. This is of a great interest in the prediction of corro fatigue crack initiation time.

4. REFERENCES

1. W. K. Jonhson, Br. Corr. J., vol. 6, (1971), 200.
2. T. G. Dunford and B. E. Wilde, in Field metallography, Failure analysis and metallography, M. E. Blum, P. M. French and G. F. Vandervoort, Metals Park, Oh, ASM, (1987), 263.
3. E. Lunarska, E. Trela and Z. Szklarska-Smialowska, Corrosion 43, (1987), 219.
4. G. S. Chen, M. Gao and R. P. Wei, Microconstituents induced pitting corrosion in a 202 aluminum alloy, to be published, 1997.
5. C. M. Liao, J.M. Olive, M. Gao and R. P. Wei, In situ monitoring of pitting corrosion in a 2 aluminum alloy, Corrosion, accepted in 1997.
6. D. G. Harlow and R. P. Wei, Probability modeling for the growth of corrosion pits, to published, 1997.
7. R. Morris and W. Smyrl, J. Electrochem. Soc., 136, (1989), 3229.
8. P. Doigt and P.E.J. Flewitt, J. Electrochem. Soc., 126, (1979), 2057.
9. E. Bardal, R. Jonhson and P.O. Gartland, Corrosion, 40, (1984), 628.
10. F. Mansfeld, Corrosion, 27, 10, (1971), 436.
11. F. Mansfeld, Corrosion, 29, 10, (1973), 403.
12. F. Mansfeld and J. V. Kenkel, in Galvanic and pitting corrosion field and laboratories stud ASTM STP 576, (1976), 20.